Near-Infrared Fluorescence Enhancement Strategy of Amorphous Silicon Nanoparticles for Night Vision Imaging and Visualizing Latent Fingerprints

Qian Zhang[1], Wanyin Ge[1,*], Yunting Wang[2], Di Han[2], Maohao Yang[1], Xin Xie[1], Peng He[1], Honglei Yin[1]

[1] *School of Materials Science and Engineering, School of Antiquities Preservation Science & Technology, Shaanxi University of Science and Technology, Xi'an, Shaanxi 710021, P. R. China.*

[2] *Materials Institute of Atomic and Molecular Science, Shaanxi University of Science and Technology, Xi'an, Shaanxi 710021, P. R. China.*

* Corresponding author. Email address: gewanyin@sust.edu.cn

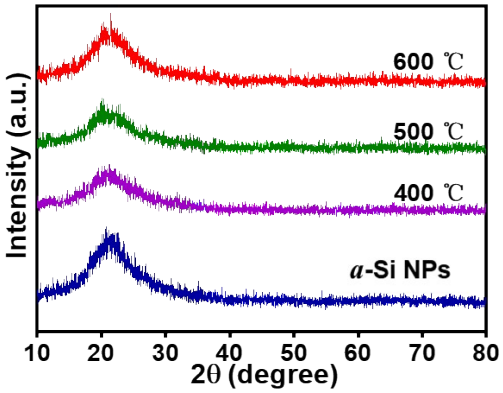

Figure S1. XRD pattern of nanoparticles annealed at various temperature.

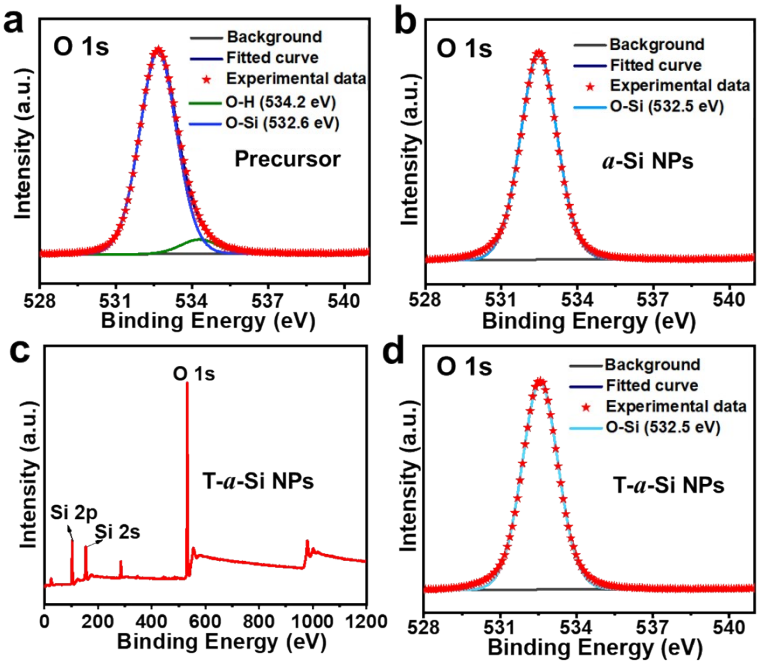

Figure S2. (a) XPS spectra of the O 1s orbital for precursor; (b) XPS spectra of the O 1s orbital for *a*-Si NPs; (c) XPS full spectra of *a*-Si NPs; (d) XPS spectra of the O 1s orbital for T-*a*-Si NPs.

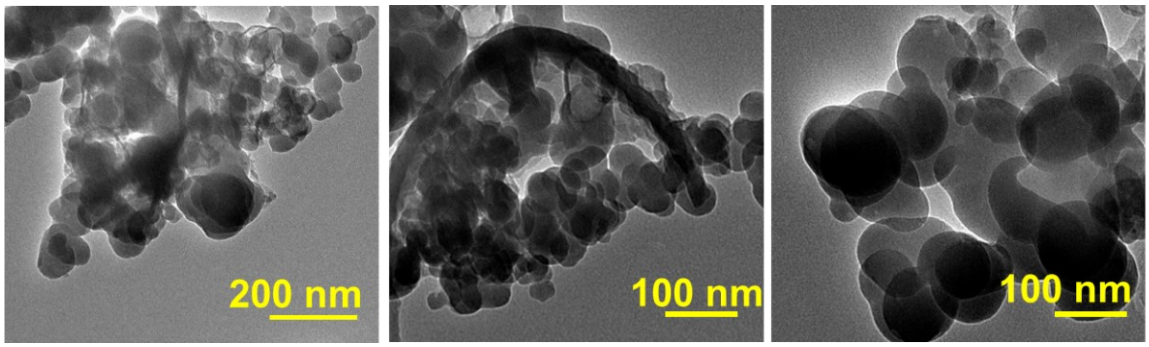

Figure S3. TEM image of the precursor.

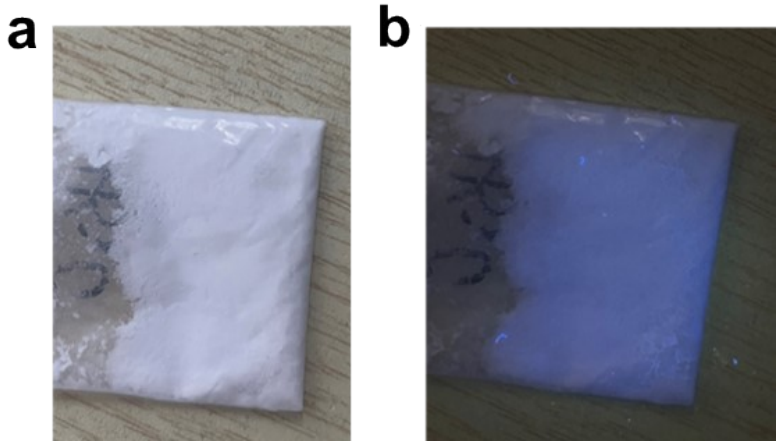

Figure S4. (a) Photographs of precursor under natural light; (b) Photographs of precursor excited by 365 nm light source.

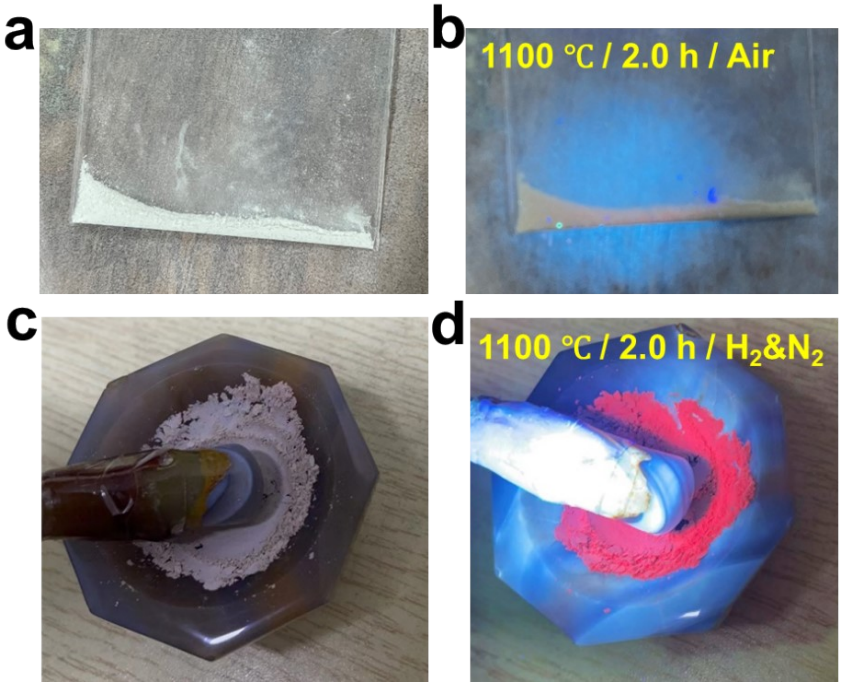

Figure S5. Annealing in air (a) Natural light; (b) Photographs excited by 365 nm light source; Annealing in a mixture of hydrogen and nitrogen (c) Natural light; (d) Photographs excited by 365 nm light source.

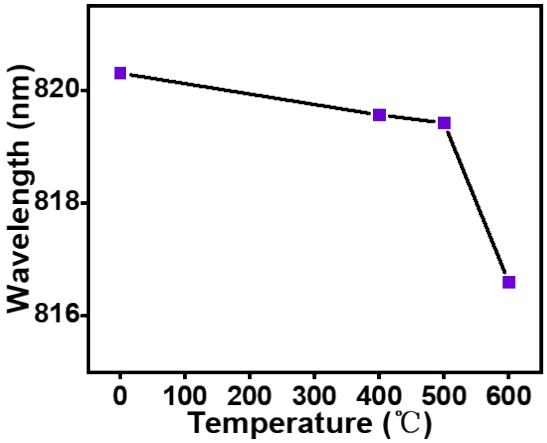

Figure S6. The dot plot of secondary annealing temperature and emission peak position.

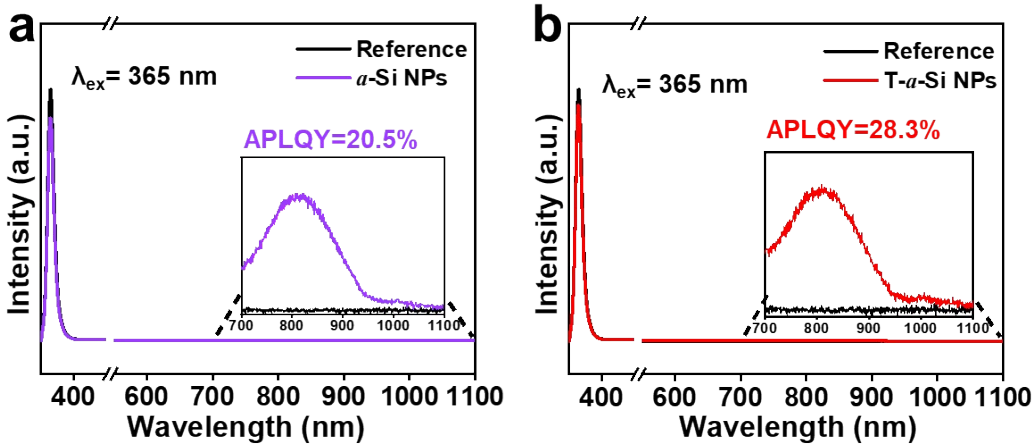

Figure S7. The absolute photoluminescence quantum yield of *a*-Si NPs and T-*a*-Si NPs.

Table S1. Comparison of fluorescence yield of different silicon nanomaterials.

Silicon nanomaterials	Synthesis method	PL emission peak (nm)	Size (nm)	PLQY (%)	Ref
Si QD	γ -ray irradiation technique	395	1.3±0.22	14.6	[1]
Au NP-Si QD	one-pot synthetic route	467	3.6	3.1	[2]
a-Si NW	electrodeposition in ionic liquids	780	110	＞25	[3]
Si QD	convert waste	680	3	21	[4]
R-Si QDs B-Si QDs	thermal hydrosilylation under argon gas	410 700	2.5±0.73 5.1±0.68	5.8 34.6	[5]
Si QD-S	self-limited self-assembly process	790	100	12.8	[6]
Metal-doped SiNCs (M=Ni, Mn, Co)	gel thermal disproportionation	992 (Ni) 985 (Mn) 1000 (Co)	8.75±3.25 7.5±1.5 7.3±1.3	5 8 26	[7]

Vinyl-POSS-ncSi	thermal hydrosilylation, thermal	850-900		11.8	[8]
a-Si NPs	sol-gel derived polymer and heat treatment	820	19-25	20.5	this work
T-*a*-Si NPs		820	18-22	28.3	

Note: Silicon quantum dot (Si QD); Amorphous Si nanowires (*a*-Si NW); Blue/ Red emission silicon quantum dot (R/B-Si QDs); Silicon quantum dot supraparticles (Si QD-S); POSS polymer composites with silicon nanocrystals (Vinyl-POSS-ncSi).

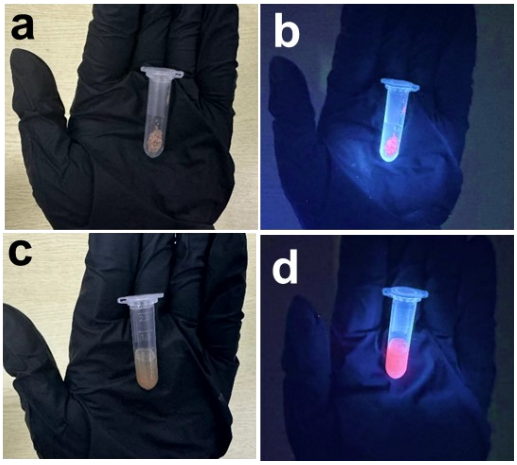

Figure S8. Photographs of T-*a*-Si NPs excited by natural light (a) and 365 nm light source (b); Photographs of T-*a*-Si NP in water under the excitation of natural light (c) and 365 nm light (d).

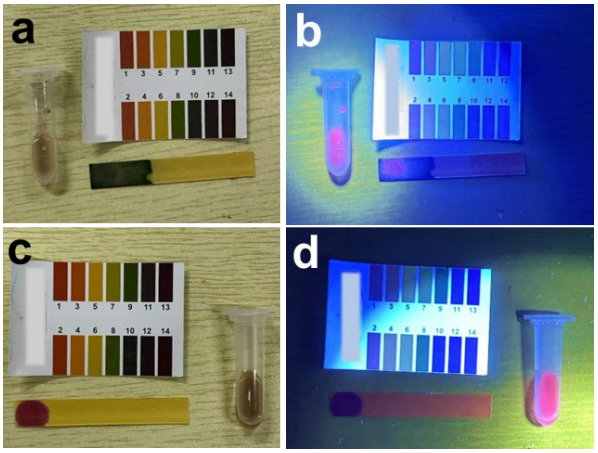

Figure S9. The pH contrast diagram of T-*a*-Si NPs in hydrochloric acid solution under the excitation of natural light (a) and 365 nm light source (b); The pH contrast diagram of T-*a*-Si NPs in ammonia aqueous solution was excited by natural light (c) and 365 nm light source (d).

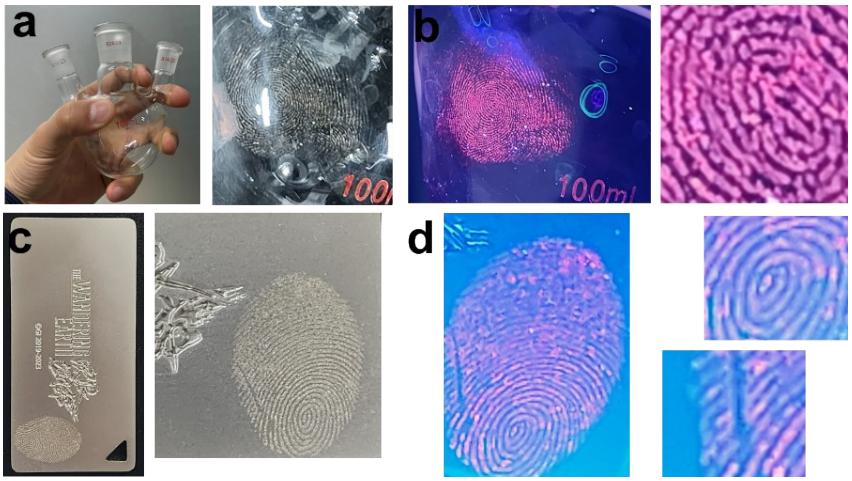

Figure S10. (a) Photos of round-bottom flask fingerprints under natural light; (b) Photographs of round-bottom flask fingerprints excited by 365 nm light source; (c) Photographs of metal card fingerprints under natural light; (d) Photographs of me tal card fingerprints excited by 365 nm light source.

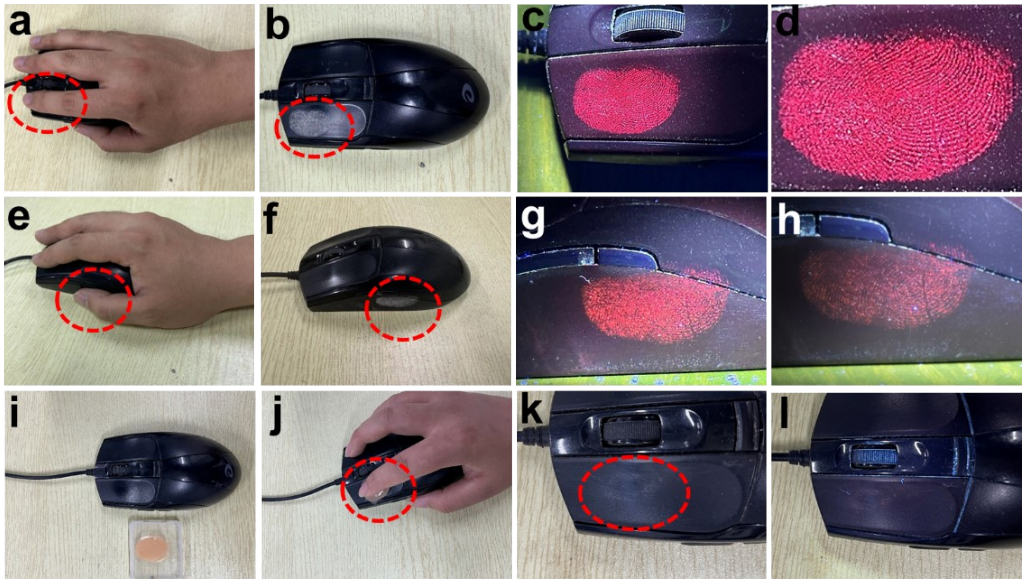

Figure S11. (a) (e) Photos of operating the mouse; (b) (f) (k) T-*a*-Si NPs powder after spraying and blowing away the floating powder; (c) (d) (g) Fingerprint photo excited by 365 nm light source; (h) The fingerprint photo excited by the 365 nm light source after blowing away part of the powder in the Figure S9j; (i) Fingerprints of mouse and silica gel mold; (j) Silica gel mold fingerprint operation mouse photos ; (l) 365 nm light source excitation k fingerprint photo.

References

1. Guleria, A.; Neogy, S.; Maurya, D. K.; Adhikari, S., Blue Light-Emitting Si Quantum Dots with Mesoporous and Amorphous Features: Origin of Photoluminescence and Potential Applications. *Journal of Physical Chemistry C* **2017,** *121* (43), 24302-24316.
2. Sharma, B.; Tanwar, S.; Sen, T., One Pot Green Synthesis of Si Quantum Dots and Catalytic Au Nanoparticle-Si Quantum Dot Nanocomposite. *Acs Sustainable*

Chemistry & Engineering **2019,** *7* (3), 3309-3318.

3. Thomas, S.; Mallet, J.; Martineau, F.; Rinnert, H.; Molinari, M., Strong Room-Temperature Visible Photoluminescence of Amorphous Si Nanowires Prepared by Electrodeposition in Ionic Liquids. *Acs Photonics* **2018,** *5* (7), 2652-2660.
4. Terada, S.; Ueda, H.; Ono, T.; Saitow, K.-i., Orange-Red Si Quantum Dot LEDs from Recycled Rice Husks. *Acs Sustainable Chemistry & Engineering* **2022,** *10* (5), 1765-1776.
5. Le, T.-H.; Le, D. T. T.; Tung, N. V., Synthesis of Colloidal Silicon Quantum Dot from Rice Husk Ash. *Journal of Chemistry* **2021,** *2021*, 6689590.
6. Fujii, M.; Fujii, R.; Takada, M.; Sugimoto, H., Silicon Quantum Dot Supraparticles for Fluorescence Bioimaging. *Acs Applied Nano Materials* **2020,** *3* (6), 6099-6107.
7. Chandra, S.; Masuda, Y.; Shirahata, N.; Winnik, F. M., Transition-Metal-Doped NIR-Emitting Silicon Nanocrystals. *Angewandte Chemie-International Edition* **2017,** *56* (22), 6157-6160.
8. Chen, D.; Sun, W.; Qian, C.; Reyes, L. M.; Wong, A. P. Y.; Dong, Y.; Jia, J.; Chen, K. K.; Ozin, G. A., Porous NIR Photoluminescent Silicon Nanocrystals-POSS Composites. *Advanced Functional Materials* **2016,** *26* (28), 5102-5110.